# 2 Chemistry

## 2-1 A New Metastable Photo-induced Phase of Cu(II) Complexes Studied by XAFS

Photoinduced (PI) phase transitions have become an attractive subject in recent years from both experimental and theoretical points of view. It has been believed that the PI phase is the same state as the thermally induced high-temperature (HT) phase. Very recently, however, Takahashi *et al.* [1] have reported a new type of PI metastable phase in $Cu(dieten)_2X_2$ (dieten=N,N-diethyl-ethylenediamine, $X$=$BF_4$ and $ClO_4$) complexes. These materials are known to exhibit thermochromic phase transitions; the low-temperature (LT) red phase consists of the planar $CuN_4$ unit, while in the HT purple phase the $CuN_4$ unit is distorted tetrahedrally. From the color change the PI transition is expected to be similar to the thermally driven phase transition; the PI phase may contain the tetrahedrally distorted $CuN_4$ unit. The powder X-ray diffraction patterns of the PI phase were, however, found to be different from the HT phase, although no correspondence between the structure and diffraction patterns was deduced. In this work, Cu K-edge XAFS spectra have been measured and analyzed in order to clarify the molecular structure in the PI phase [2].

The powdered thin sample was irradiated by UV light from an Hg lamp for 5-10 minutes at 30 K (see Experimental Setup in Fig. 1). Cu K-edge XANES spectra [Fig. 1(a)] measured at BL-9A show that the Cu1s-to-4pπ tran-

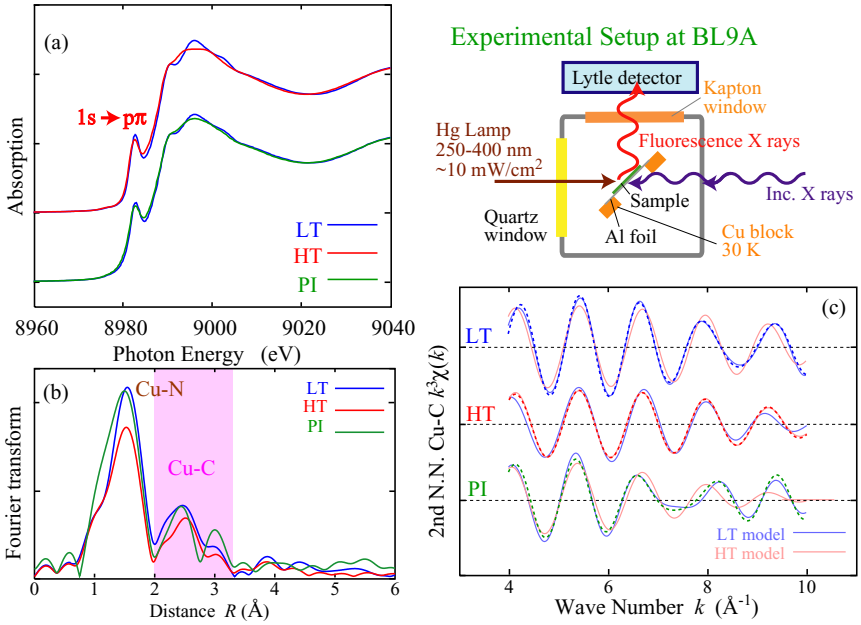


Figure 1
(a) Cu K-edge XANES of the LT, HT and PI phases. (b) Fourier transforms of the EXAFS function $k^3\chi(k)$. (c) Filtered $k^3\chi(k)$ and the fitting results. The experimental setup is also depicted. These results are those for the $ClO_4$ salt, and those for $BF_4$ are essentially the same.

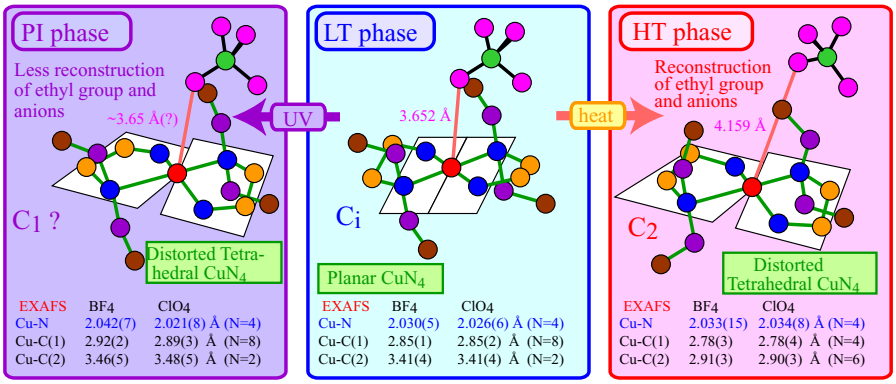


Figure 2
Proposed structure transformation in the PI phase transition.

sition was found to be weakened and the spectral features at 8990-9005 eV smeared out in both the thermally-driven and photoinduced transitions, implying that the $CuN_4$ unit in the PI phase is distorted tetrahedrally, in a similar manner to the HT phase. In comparison, EXAFS shows a different finding, however, in the second-nearest neighbor Cu-C shells [see Fig. 1(b)]. As shown in Fig. 1(c), the filtered $k^3\chi(k)$ of the PI phase can be fitted much better by using the LT model as a standard. This implies that the configuration of the surrounding C atoms in the PI phase is closer to the LT phase than to the HT phase.

We can conclude that the PI phase is a new metastable state, whose intramolecular structure is not equivalent to that of either the HT or LT phase. The $CuN_4$ unit exhibits tetrahedral distortion, while the atomic configuration of the ethylene and ethyl groups is similar to those of the LT phase. One can thus propose a possible model structure as shown in Fig. 2. The $Cu(dieten)_2$ ion has an inversion center in the LT phase (point group $C_i$) and a $C_2$ axis in the HT phase (point group $C_2$). We can suppose that when the LT phase is transformed to the PI phase upon UV irradiation, the $CuN_4$ plane is distorted tetrahedrally with less reconstruction of the dieten ligand than on the LT phase. This should be a reasonable hypothesis since the transformation of the configuration of the ethyl groups and also the anions would require too much activation energy to complete at such low temperatures as 30 K.

**T. Yokoyama[1], K. Takahashi[2] and O. Sato[2] ([1]IMS, [2]KAST)**

## References

[1] K. Takahashi, R. Nakajima, Z.-Z. Gu, H. Yoshiki, A. Fujishima and O. Sato, *Chem. Commun.* (2002) 1578.
[2] T. Yokoyama, K. Takahashi and O. Sato, *Phys. Rev. B* **67** (2003) 172104.

# 2-2 Novel Crystal Growth from Titania Nanosheets Studied by Total Reflection Fluorescence XAFS

Nanomaterials have recently attracted intense interest from both fundamental and practical points of view. These materials offer intriguing physical and chemical properties associated with their size and shape on a nanometer scale. Examples of these properties include size-quantization effects for semiconductor nanocrystallites [1], and the helicity-dependent semiconducting/metallic properties of carbon nanotubes [2]. Many novel phenomena peculiar to the nanoscopic regime are expected to be as yet undiscovered.

We report here a thermally-induced structural change observed in a monolayer film of titania nanosheets using a total reflection fluorescence X-ray absorption fine structure (TR-FXAFS) technique, which can provide high sensitivity for these ultrathin inorganic system [3].

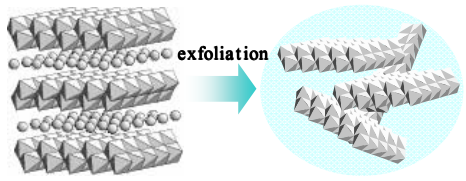


Figure 3
Schematic explanation for nanosheet formation via exfoliation of a layered titanate.

Titania nanosheets of $Ti_{1-\delta}O_2^{4\delta-}$ ($\delta \approx 0.09$) were obtained by delaminating a layered titanate, $H_{0.7}Ti_{1.825}X_{0.175}O_4 \cdot H_2O$ ($X$ = vacancy), into colloidal single layers (Fig. 3) [4]. The resulting two-dimensional crystallites had a molecular thickness of ~0.7 nm, and consisted of two edge-shared $TiO_6$ octahedra. In contrast, the lateral dimensions of the crystallites ranged from several hundred nanometers to several micrometers. A monolayer film of these titania nanosheets was deposited by electrostatic self-assembly onto quartz glass substrates precoated with a cationic polymer [5]. The resultant films were heated to 600, 700, 800 and 900°C for 1 hour. TR-FXAFS spectra were obtained at BL-9A and 12C, equipped with Si(111) double-crystals and 19 element Ge-solid state detectors with s- and p-polarization geometrical arrangements. Ti K-edge X-ray Absorption Near-Edge Structure (XANES) spectra were obtained over an energy range from 4944 to 5020 eV at an interval of 0.3 eV at room temperature.

Figure 4 shows normalized Ti-K-edge XANES spectra (s-polarization) for an as-grown monolayer film of titania nanosheets and also for the heat-treated samples. There is no marked change in the XANES spectra below

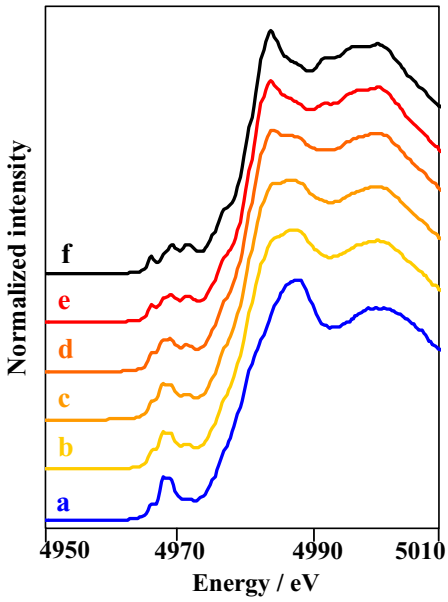


Figure 4
Normalized Ti-K XANES spectra for (a) as-grown film and for samples heated at (b) 600°C, (c) 700°C, (d) 800°C and (e) 900°C. The data for (f) anatase is also shown for a reference.

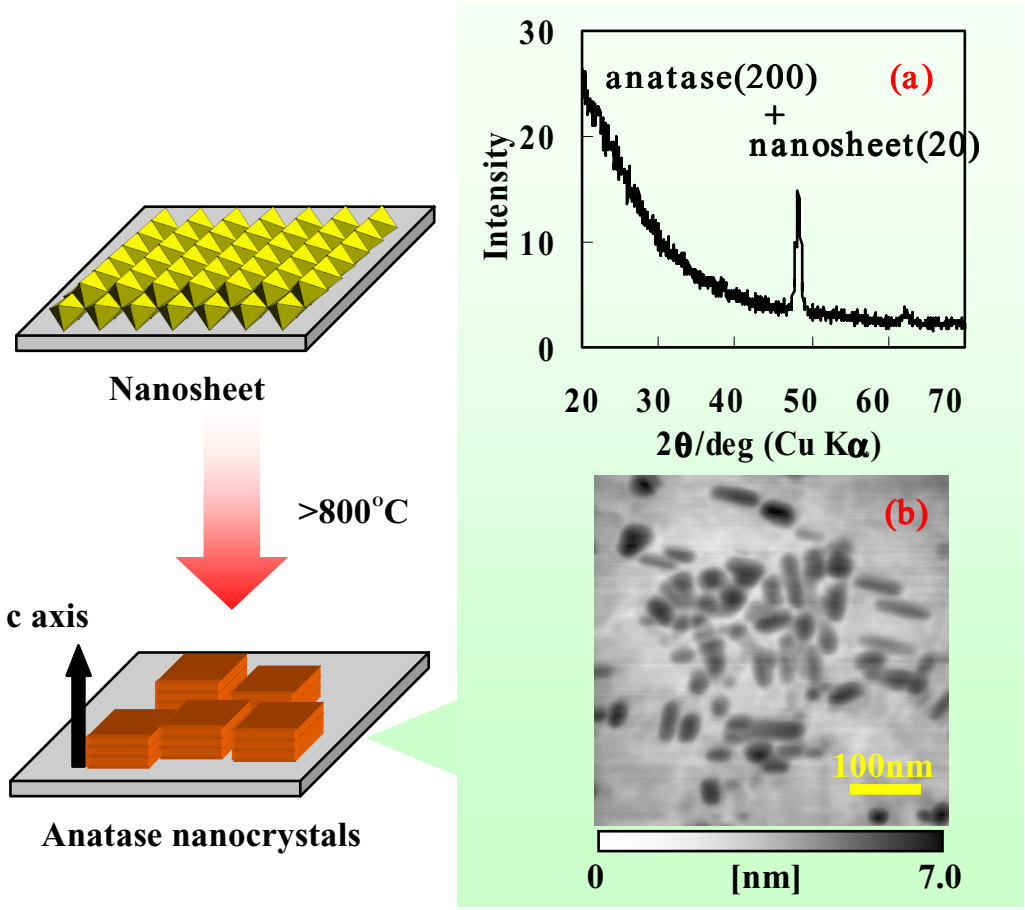


Figure 5
Novel crystallization of anatase nanocrystals from a monolayer film of titania nanosheets: (a) in-plane diffraction pattern and (b) AFM image of anatase nanocrystals.

700ºC except for a slight change in the white-line region. Peaks characteristic of anatase [Fig. 4(f)] appear above 700ºC. A sharp white-line peak at 4984 eV and also fine structures at the pre-edge region were clearly observed at this temperature. Upon further heating to 900ºC, the spectrum (e) was identifiable as a single phase of anatase. This result suggests that the nanosheets started to change into anatase at 800ºC, and that the transformation was complete by 900ºC. Remarkably, in-plane X-ray diffraction data for the film heated to 800ºC [Fig. 5(a)] show only one peak, indexable to the 200 reflection of anatase. This suggests a preferred orientation of anatase along the c-axis with respect to the substrate surface, although the peak contains 20 reflection of the nanosheet for a face-centered two-dimensional unit cell (0.38 nm × 0.30 nm). Atomic force microscopy observations reveal anatase crystallites with a lateral size of about 100 nm × 50 nm and a height of 3-5 nm [Fig. 5(b)].

This crystallization behavior is distinct from that observed for bulk titania-based materials. The crystallization temperature is higher by at least 300ºC, and growth is preferentially along a particular crystallographic axis. This may be assumed to be due to the difference in the starting atomic configurations. Since the nanosheet crystallite has only two planes of Ti atoms and four planes of O atoms, the nucleation of anatase from such a thin system requires extensive diffusion of the atoms, needing a much higher temperature than usual. This behavior has been more quantitatively elucidated by the analysis of polarized EXAFS data and the results will be reported elsewhere. This finding may be considered to be a novel phenomenon peculiar to two-dimensionally bound nanoscopic systems.

The present study suggests that it is possible to fabricate an ultrathin oriented crystalline phase of titania on a desired substrate. This will open up a new application field for titania, one of the most important high-tech materials. The structure of titania nanosheets has been clarified for the first time through this study. Such information will be essential for understanding the unique physical properties of the titania nanosheets [1].

**K. Fukuda[1,2], I. Nakai[1], M. Harada[2] and T. Sasaki[2,3]**
**([1]Tokyo Univ. of Sci., [2]NIMS, [3]CREST/JST)**

## References

[1] T. Sasaki and M. Watanabe, *J. Phys. Chem. B* **101** (1997) 10159.
[2] S. Iijima, *Nature* **354** (1991) 56.
[3] K. Fukuda, T. Sasaki, M. Watanabe, I. Nakai, K. Inaba and K. Omote, *Cryst. Growth & Design* **3** (2003) 281.
[4] T. Sasaki, M. Watanabe, H. Hashizume, H. Yamada and H. Nakazawa, *J. Am. Chem. Soc.* **118** (1996) 8329.
[5] T. Sasaki, Y. Ebina, M. Watanabe and G. Decher, *Chem. Commun.* (2000) 2163.

## 2-3 Charge-Discharge Reaction Mechanism of High Capacity Oxide-Anode-Materials for Li Secondary Battery

During the last three decades, enormous research and development efforts have been undertaken in the search for a viable rechargeable battery system with more advanced performance than the lead-acid battery. These efforts were motivated by changing requirements for power systems, *e.g.*, portable computers, computer memory preservation, and mobile telephones. Under these circumstances, an epoch-making novel battery system was proposed. This was the Li battery, which has high energy density and high output potential. Commercially available lithium ion batteries generally employ graphitized carbon as the anode material. However capacity is limited to about 370 Ah/kg which is substantially smaller than that of metallic lithium, and rate properties are not always enough for consideration as the anode for large-scale batteries of the future. In order to overcome these problems, a novel anode material for a lithium ion secondary battery, $MnV_2O_6$, was prepared [1]. X-ray absorption fine structure (XAFS) spectra on the Mn and V K-edges were measured in a transmission mode at room temperature on BL-9A to study electrochemical properties of $MnV_2O_6$ [2,3].

X-ray diffraction (XRD) analysis indicated that $MnV_2O_6$ has a brannerite type structure. Figure 6 shows the charge-discharge profiles of $MnV_2O_6$ at the first and second cycles [3]. Solid circles represent the voltages at which XAFS measurements of the electrodes were carried out. The profiles in the figure indicate that the first charge (Li insertion in $MnV_2O_6$) shows a large capacity of about 1000 Ah/kg, which is much larger than that of graphite.

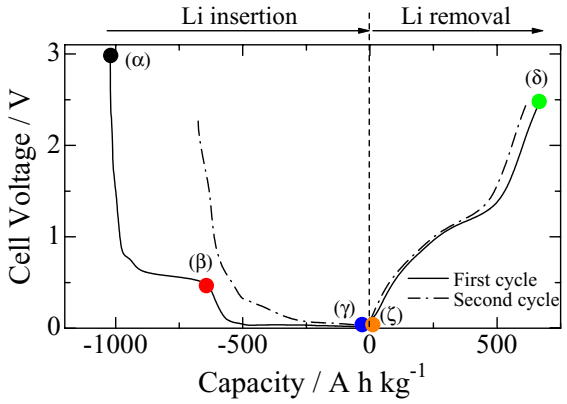


Figure 6
The first and second charge-discharge curves of $MnV_2O_6$. Solid circles represent the cell voltage (α) before electrochemical measurement, (β) at 0.40 V during the charge process, (χ) at 0.01 V during the charge process, (δ) at 2.5 V during the discharge process, and, (ε) at 0.01 V during the second charge process.

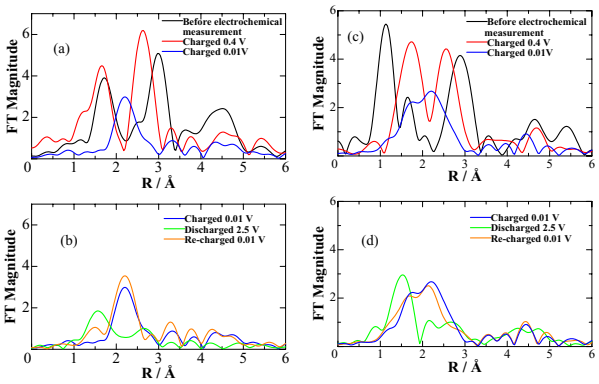


Figure 7
Fourier transforms of the Mn K-edge EXAFS (a,b) and V K-edge EXAFS (c,d) spectra for the electrodes at various voltages. (a,c); the first charge, (b,d); following discharge and re-charge.

Figure 7 shows the Fourier transforms of the Mn K-edge [(a,b)] and V K-edge [(c,d)] EXAFS spectra for the electrode at various potentials during the first lithium insertion [(a,c)] and following extraction and re-insertion [(b,d)] [3]. In the case of the electrode before electrochemical measurement in Fig. 7(a), the first peak located around 1.7 Å corresponds undoubtedly to Mn-O distances and the second one centered at 3.0 Å can be attributed to the Mn-Mn and/or the Mn-V distance. The Fourier transforms for Mn and V indicate that the local environmental structure around the transition metals reversibly changes during the cycles, even though the long-range structure cannot be observed by XRD after the first charge. However, the local environments at 2.5 V during the discharge (δ) for both Mn and V in the active material differ from those in the $MnV_2O_6$ electrode before electrochemical measurement (α). This phenomenon accounts for the irreversible capacity in the first cycle, which is observed in Fig. 6, because of the different lattice potentials between the electrode before electrochemical measurement and at 2.5 V during discharge. It can be concluded that controlling the local structure around the transition metals is an effective way of improving anode properties.

**Y. Uchimoto (Tokyo Inst. of Tech.)**

### References

[1] D. Hara, H. Ikuta, Y. Uchimoto and M. Wakihara, *J. Mater. Chem.* **12** (2002) 2507.
[2] D. Hara, J. Shirakawa, H. Ikuta, Y. Uchimoto, M. Wakihara, T. Miyanaga and I. Watanabe, *J. Mater. Chem.* **13** (2003) 897.
[3] D. Hara, J. Shirakawa, H. Ikuta, Y. Uchimoto, M. Wakihara, T. Miyanaga and I. Watanabe, *J. Mater. Chem.* **12** (2002) 3717.